Proc. Indian Acad. Sci. (*Chem. Sci.*), Vol. 111, No. 5, October 1999, pp. 627–637

A synthetic iron phosphate mineral, spheniscidite, $[NH_4]^+[Fe_2(OH)(H_2O)(PO_4)_2]^-H_2O$, exhibiting reversible dehydration

AMITAVA CHOUDHURY[#1] and SRINIVASAN NATARAJAN[#]*
[#]Chemistry and Physics of Materials Unit, Jawaharlal Nehru Centre for Advanced Scientific Research, Jakkur PO, Bangalore 560 064, India
[1]Solid State and Structural Chemistry Unit, Indian Institute of Science, Bangalore 560 012, India
e-mail: raj@jncasr.ac.in

MS received 16 April 1999

Abstract. Spheniscidite, a synthetic iron phosphate mineral has been synthesized by hydrothermal methods. The material is isotypic with another iron phosphate mineral, leucophosphite. Spheniscidite crystallizes in the monoclinic spacegroup $P2_1/n$. ($a = 9{\cdot}845(1)$, $b = 9{\cdot}771(3)$, $c = 9{\cdot}897(1)$, $\beta = 102{\cdot}9°$, $V = 928{\cdot}5(1)$, $Z = 4$, $M = 372{\cdot}2$, $d_{calc} = 2{\cdot}02$ g cm^{-3} and $R = 0{\cdot}02$). The structure consists of a network of FeO_6 octahedra vertex-linked with PO_4 tetrahedra forming 8-membered one-dimensional channels in which the NH_4^+ ions and H_2O molecules are located. The material exhibits reversible dehydration and good adsorption behaviour. Magnetic susceptibility measurements indicate that the solid orders antiferromagnetically.

Keywords. Open-framework materials; adsorption; reversible dehydration; antiferromagnetism; structure-directing agents.

1. Introduction

Open-framework materials continue to be of interest due to their potential applications in catalysis, sorption and separation processes[1]. A number of structurally-diverse materials having open-framework architecture have been synthesized and characterized[2]. Of these, iron phosphates in particular, have been studied with interest due to their rich crystal chemistry. One of the naturally occurring iron phosphate minerals, cacoxenite, possesses an extra-large channel of 14·2 Å filled with water molecules[3]. These materials are constructed from the networking of FeO_6 octahedra and PO_4 tetrahedra. There is considerable incentive for the synthesis of new open-framework iron phosphate materials due to their potential application in the oxidative dehydrogenation of isobutyric acid to methacrylic acid which is used as a raw material for various polymers[4]. The synthesis and structures of several iron phosphates prepared in the presence of organic amines have been recently reviewed[5]. Most of these materials are made under hydrothermal conditions. During the course of a program to investigate new solids formed in the presence of structure-directing agents (SDA's), we have obtained a synthetic iron phosphate mineral, spheniscidite; $[NH_4]^+[Fe_2(OH)(H_2O)(PO_4)_2]^-H_2O$, the structure of

*For correspondence

which was recently reported[6]. The structure of spheniscidite possesses two 8-membered channels where the $[NH_4]^+$ and one half of the water molecules are located. The structure of the mineral is closely related to another iron phosphate mineral, leucophosphite $[KFe_2(PO_4)_2OH]\cdot 2H_2O$[7]. The physical properties of the synthetic spheniscidite, especially its adsorptive behaviour, have not been investigated. We have carried out a systematic investigation on the dehydration–hydration processes of the water molecules and ion-exchange properties of the $[NH_4]^+$ ions that are present in the channels of this mineral. The results show that the solid undergoes reversible dehydration–hydration process without any perceptible change in the structure and also shows adsorptive properties akin to those of aluminosilicate zeolites.

2. Experimental

2.1 *Synthesis and initial characterization*

The title compound was made under mild hydro/solvothermal conditions. In a typical synthesis, 0·1663 g of iron oxide was added to a mixture of water (1·5 ml) and glycol (3 ml, EG). To this solution, 0·57 ml of aqueous phosphoric acid (85 wt%) and 0·149 ml of HF was added under stirring. To this 0·54 ml of 1,3-diaminopropane (DAP) was added and the mixture was stirred until homogeneous. The mixture was sealed in a PTFE-lined stainless-steel autoclave and heated initially at 150°C for 72 h. Another 4·5 ml of water was added and the mixture was heated to 170°C for a further period of 64 h. The final composition of the mixture was 1·0 Fe_2O_3 : 8·33 H_3PO_4 : 6·24 DAP : 4·16 HF : 333 H_2O : 52 EG. At the end of the above reaction, large quantities of transparent light yellow rhomb-like crystals resulted along with a small quantity of white powder. The crystals were easily separated using sonification in aqueous medium and used for further studies. The addition of HF was to act as a mineralizer, and ethylene glycol was added to control the vapour pressure inside the reaction vessel. It is to be noted that the same material has been obtained by the use of other structure-directing amines such as guanidine and 1,3-diaminoguanidine. The initial characterization was carried out using powder X-ray diffraction and thermogravimetric analysis (TGA).

2.2 *Single crystal structure determination*

A suitable rhomb-like single crystal of the title compound was carefully selected under a polarizing microscope and mounted at the tip of a glass fiber using cyanoacrylate (superglue) adhesive. Crystal structure determination by X-ray diffraction was performed on a Siemens Smart-CCD diffractometer equipped with a normal focus, 2·4 kW sealed tube X-ray source (MoKα radiation, $\lambda = 0{\cdot}71073$ Å) operating at 50 kV and 40 mA. A hemisphere of intensity data was collected at room temperature in 1321 frames with ω scans (width of 0·30° and exposure time of 10 s per frame) in the range $5 \le 2\theta \le 46{\cdot}5$. A total of 3741 reflections were collected in the range $-10 \le h \le 10$, $-6 \le k \le 10$, $-10 \le l \le 10$ and were merged to give 1330 unique reflections ($R_{int} = 0{\cdot}035$) of which 1230 were considered to be observed [$I > 2\sigma(I)$]. Pertinent details for the structure determination are listed in table 1.

The structure was solved by direct methods using SHELXS-86[8] and difference Fourier syntheses. No absorption correction was applied. All the hydrogen positions were found in the difference Fourier maps and for the final refinement the hydrogen atoms on the

Table 1. Crystal data and structure refinement parameters for $[NH_4]^+[Fe_2(OH)(H_2O)(PO_4)_2]^-H_2O$.

Empirical formula	$Fe_2P_2O_{11}N_1H_9$
Crystal system	Monoclinic
Space group	$P2_1/n$
Crystal size (mm)	0·08 × 0·08 × 0·08
a (Å)	9·845(1)
b (Å)	9·771(3)
c (Å)	9·897(1)
α (°)	90·0
β (°)	102·8(1)
γ (°)	90·0
Volume (Å^3)	928·5(1)
Z	4
Formula mass	372·7
ρ_{calc} (gcm^{-3})	2·02
λ (MoKα) Å	0·71073
μ (mm^{-1})	2·65
θ range (°)	2·64–23·22
Total data collected	3741
Index ranges	$-10 \le h \le 10$, $-6 \le k \le 10$, $-10 \le 1 \le 10$
Unique data	1330
Observed data ($\sigma > 2\sigma(I)$)	1230
Refinement method	Full-matrix least-squares on $\|F^2\|$
R indexes [$I > 2\sigma(I)$]	R_1 = 0·022[a], wR_2 = 0·054[b]
R indexes (all data)	R_1 = 0.026, wR_2 = 0·056
Goodness of fit (S)	1·15
No. of variables	181
Largest difference map peak and hole eÅ^{-3}	0·468 and –0·598

[a] $R_1 = \sum \|\|F_0\| - \|F_c\|\| / \sum |F_0|$; [b] $wR_2 = \{\sum[w(F_0^2 - F_c^2)^2] / \sum[w(F_0^2)^2]\}^{1/2}$. $w = 1/[\sigma^2(F_0)^2 + (aP)^2 + bP]$, $P = [\max(F_0^2, 0) + 2(F_c)^2]/3$, where a = 0·014 and b = 2·559

Table 2. Atomic coordinations [× 10^4] and equivalent isotropic displacement parameters [Å^2 × 10^3] for $[NH_4]^+[Fe_2(OH)(H_2O)(PO_4)_2]^-H_2O$.

Atom	x	y	z	U(eq)[#]
Fe(1)	1019(1)	7317(1)	8133(1)	6(1)
Fe(2)	–1133(1)	10447(1)	8698(1)	7(1)
P(1)	–2036(1)	9652(1)	11480(1)	6(1)
P(2)	–2076(1)	8167(1)	6314(1)	7(1)
O(1)	2376(2)	6690(2)	9752(2)	12(1)
O(2)	–549(2)	7716(3)	6580(2)	12(1)
O(3)	1878(2)	6305(2)	6832(2)	11(1)
O(4)	2135(2)	8937(2)	7850(2)	11(1)
O(5)	–2052(2)	12154(2)	8048(2)	11(1)
O(6)	–2374(2)	9820(2)	9881(2)	9(1)
O(7)	–2186(2)	9585(2)	6993(2)	10(1)
O(8)	550(2)	10930(2)	8014(2)	9(1)
O(9)	16(3)	8594(3)	9401(3)	8(1)
O(10)	–55(4)	5542(3)	8447(3)	21(1)
O(100)	1805(3)	3535(3)	9647(4)	27(1)
N(1)	5109(4)	8104(4)	8969(4)	21(1)

[#] U(eq) is defined as one third of the trace of the orthogonalized U_{ij} tensor

amine molecule were placed geometrically and held in the riding mode. The last cycles of refinement included atomic positions, anisotropic thermal parameters for all the non-hydrogen atoms and isotropic thermal parameters for all the hydrogen atoms. Full-matrix-least-squares structure refinement against $|F^2|$ was carried out using SHELXTL-PLUS[9] package of programs. The final Fourier map had minimum and maximum peak of –0·598 and 0·468 eÅ^{-3}. Final R values, $R = 0{\cdot}022$ and $R_w = 0{\cdot}054$ and S = 1·15 were obtained for a total of 181 parameters. The final atomic coordinates and selected bond distances and angles are presented in tables 2 and 3.

3. Results and discussion

The synthetic spheniscidite, $[NH_4]^+[Fe_2(OH)(H_2O)(PO_4)_2]^-H_2O$, has been synthesized by hydrothermal methods and the structure determined by single crystal methods. Since the synthesis involves kinetically controlled solvent-mediated reactions, there is no apparent correlation between the starting composition and the stoichiometry of the solid product. The asymmetric unit presented in figure 1 contains 16 non-hydrogen atoms of which 14 belong to the 'framework' (2 Fe, 2 P and 10 O atoms) and 2 to the guest (1 N and 1 O atoms).

Table 3. Selected bond distances and angles for $[NH_4]^+[Fe_2(OH)(H_2O)(PO_4)_2]^-H_2O$.

Moiety	Distance (Å)	Moiety	Distance (Å)
Fe(1)–O(1)	1·944(2)	Fe(2)–O(9)	2·167(3)
Fe(1)–O(2)	1·962(2)	Fe(2)–O(9)$^{\#1}$	2·171(3)
Fe(1)–O(3)	1·958(2)	P(1)–O(3)$^{\#2}$	1·518(2)
Fe(1)–O(4)	1·982(2)	P(1)–O(4)$^{\#1}$	1·543(3)
Fe(1)–O(9)	2·157(3)	P(1)–O(8)$^{\#1}$	1·547(2)
Fe(1)–O(10)	2·090(3)	P(1)–O(6)	1·552(2)
Fe(2)–O(5)	1·938(2)	P(2)–O(1)$^{\#3}$	1·527(2)
Fe(2)–O(6)	1·967(2)	P(2)–O(2)	1·533(2)
Fe(2)–O(7)	1·964(2)	P(2)–O(5)$^{\#4}$	1·534(3)
Fe(2)–O(8)	1·980(2)	P(2)–O(7)	1·554(2)
Moiety	**Angle (°)**	**Moiety**	**Angle (°)**
O(1)–Fe(1)–O(3)	93·7(1)	O(5)–Fe(2)–O(7)	88·0(1)
O(1)–Fe(1)–O(2)	170·6(1)	O(5)–Fe(2)–O(6)	99·2(1)
O(3)–Fe(1)–O(2)	87·9(1)	O(7)–Fe(2)–O(6)	95·7(1)
O(1)–Fe(1)–O(4)	93·8(1)	O(5)–Fe(2)–O(8)	92·6(1)
O(3)–Fe(1)–O(4)	88·6(1)	O(6)–Fe(2)–O(8)	162·6(1)
O(2)–Fe(1)–O(4)	95·5(1)	O(7)–Fe(2)–O(8)	97·5(1)
O(1)–Fe(1)–O(9)	91·3(1)	O(5)–Fe(2)–O(9)	176·3(1)
O(3)–Fe(1)–O(9)	174·0(1)	O(7)–Fe(2)–O(9)	93·2(1)
O(2)–Fe(1)–O(9)	87.6(1)	O(6)–Fe(2)–O(9)	84·1(1)
O(4)–Fe(1)–O(9)	87·7(1)	O(8)–Fe(2)–O(9)	83·8(1)
O(1)–Fe(1)–O(10)	83·9(1)	O(5)–Fe(2)–O(9)$^{\#1}$	91·5(1)
O(3)–Fe(1)–O(10)	89·1(1)	O(7)–Fe(2)–O(9)$^{\#1}$	178·6(1)
O(2)–Fe(1)–O(10)	86·8(1)	O(6)–Fe(2)–O(9)$^{\#1}$	83·2(1)
O(4)–Fe(1)–O(10)	176·7(1)	O(8)–Fe(2)–O(9)$^{\#1}$	83·8(1)
O(9)–Fe(1)–O(10)	94·7(1)	O(9)–Fe(2)–O(9)$^{\#1}$	87·4(1)

$^{\#1}-x, -y+2, -z+2$; $^{\#2}x-1/2, -y+3/2, z+1/2$; $^{\#3}x-1/2, -y+3/2, z-1/2$; $^{\#4}x+1/2, -y+3/2, z+1/2$

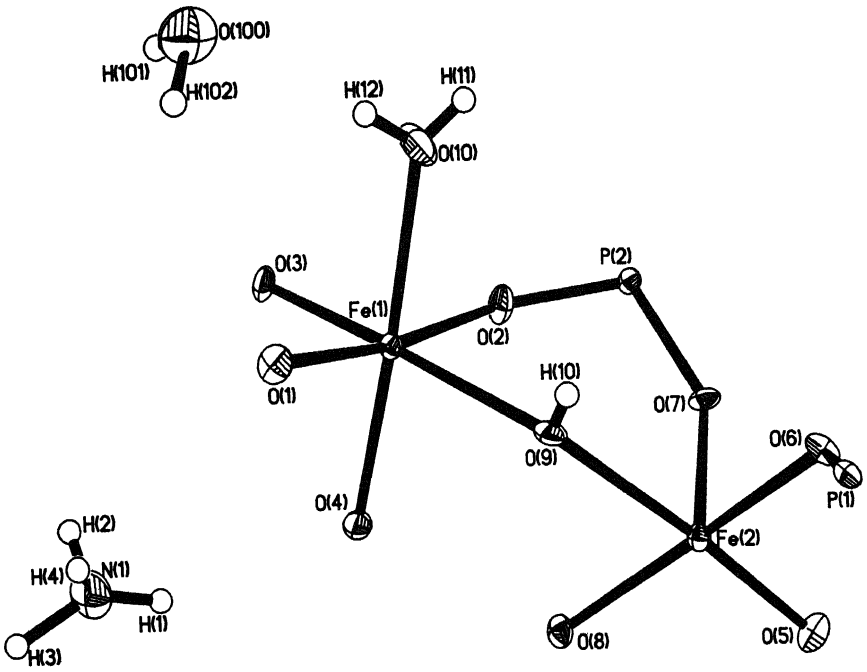

Figure 1. ORTEP plot of $[NH_4]^+[Fe_2(OH)(H_2O)(PO_4)_2]^-H_2O$. The termal ellipsoids are given at 50% probability.

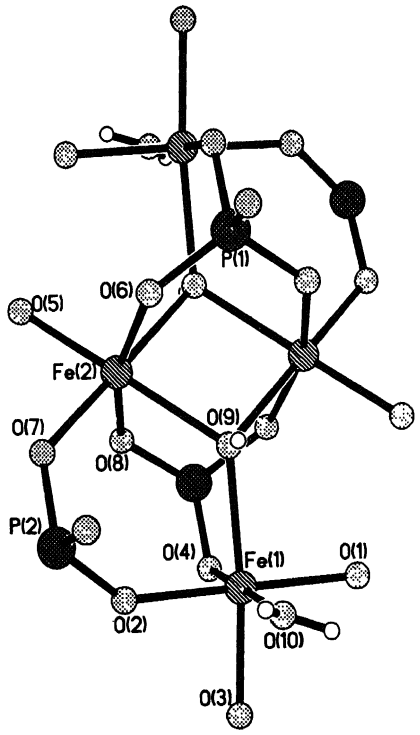

Figure 2. The basic building unit present in $[NH_4]^+[Fe_2(OH)(H_2O)(PO_4)_2]^-H_2O$. Note that the Fe atoms form a tetramer. Ammonium and water molecules are not shown.

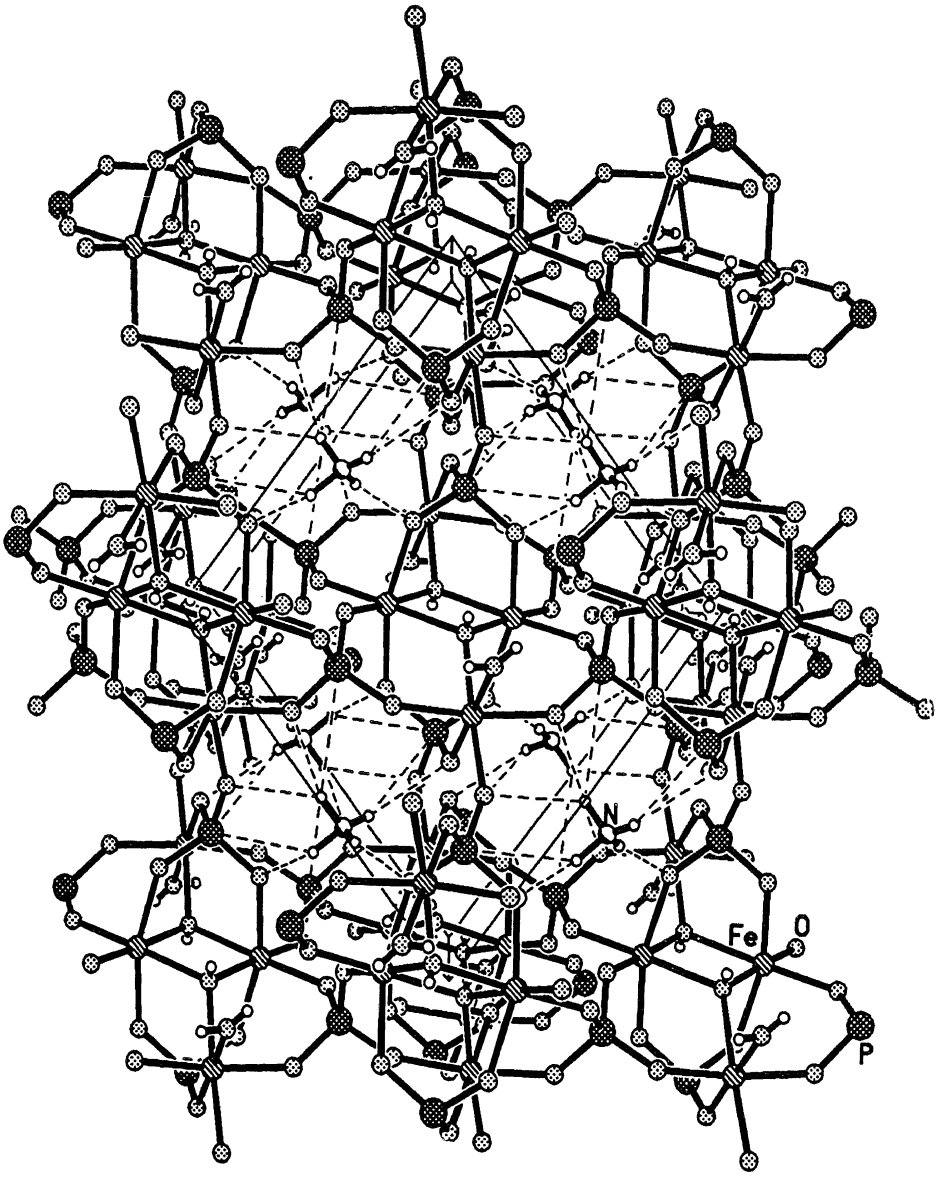

Figure 3. Structure of $[NH_4]^+[Fe_2(OH)(H_2O)(PO_4)_2]^-H_2O$ showing the one-dimensional channels along the [010] direction. The dotted lines indicate the various hydrogen bond interactions in the solid.

The structure is made from a three-dimensional covalently bonded framework built up from FeO_6 octahedra and phosphate tetrahedra. The basic building unit in the title compound is a tetramer made from FeO_6 octahedra and is shown in figure 2. The basic building unit consists of two central FeO_6 octahedra [Fe(2)] that share a common edge via an –OH group [O(9)] which are linked further to two additional FeO_6 octahedra [Fe(1)] via the corners. Thus, the edge and corner-sharing FeO_6 octahedra form a tetramer of formula Fe_4O_{20}. The phosphate tetrahedra are linked to the tetramers via the vertices (figure 2). Similar linkages have been observed earlier in a three-dimensional

iron phosphate[10] and also in the iron phosphate mineral leucophosphite, $K_2[Fe_4(OH)_2(H_2O)_2(PO_4)_2]\cdot 2H_2O$[7].

The connectivity between the FeO_6 octahedra and the PO_4 tetrahedra creates a 8-membered channel along the [010] direction (figure 3). Alternatively it may be considered that the basic building unit, the Fe tetramer, is connected to each other via the phosphate groups forming the channels (5·24 × 6·37 Å; longest atom–atom contact distance, not including the van der Waals radii). Ammonium ions and water molecules reside in these channels. The ammonium ions resulted from the decomposition of the 1,3-diaminopropane molecule used in the starting synthesis mixture as the structure-directing agent. This type of behaviour is not uncommon in open-framework materials synthesized under hydrothermal conditions and many examples exist in the literature[11]. Along the [001] direction, the connectivity between the tetramer and the phosphates creates another 8-membered channel of dimension 6·61 × 6·34 Å into which the bound water molecules extend (figure 4).

Spheniscidite has one oxygen atom connected to three Fe atoms [one Fe(1) and two Fe(2)]. Such a trigonal coordination of the oxygen atom forming Fe–O–Fe bridge is an electrostatic valence requirement of the bridging oxygen atoms. There are other examples of such electrostatic valence requirements of oxygens known in the literature[12–16]. The trigonal and tetrahedral coordinations of the oxygen atoms in open-framework studies reported in the literature[12–16] suggest that these bridges usually occur when divalent atoms are involved. It is therefore to be expected that the presence of such features in the iron phosphate system would lead to novel framework topologies which have no structural counterparts in aluminosilicates or aluminophosphates.

The iron atoms, as mentioned earlier, are hexa-coordinated forming octahedra. The Fe–O bond distances lie in the range 1·938–2·171 Å (ave. 2·023 Å), and the O–Fe–O bond angles are in the range 83·2–178·6° (table 3). These are typical values observed for iron in octahedral coordination[4,6,7,10]. From the bond angles it is clear that the Fe(1) is having a more regular octahedra than Fe(2). The longest bond distances, however, is observed for 3-coordinated oxygen atoms [O(9)] and the bound water molecules [O(10)]. The P–O distances are within the range 1·518–1·554 Å (ave. 1·539 Å) and O–P–O bond angles are in the range 107·2–111·8° (ave. 109·5°) (table 3). These values, too, are comparable to other P–O distances and angles found in many of the open-framework phosphate materials reported in the literature[9–18]. The framework density[17] (number of tetrahedral/octahedral framework atoms in 1000 $Å^3$) for this material is 17·2, indicating a degree of openness comparable to aluminophosphate molecular sieves such as AlPO-5[17].

Hydrogen bond interactions between the framework and the structure-directing agents play an important role in the formation and structural stability of many of the framework solids, especially when dealing with low dimensional materials. In the present solid, hydrogen bond interactions between the framework and the guest molecule play a crucial role as seen from table 4. It is clear that the water and the ammonium ions (guest species) present in the channels participate actively in hydrogen bonding more effectively than the –OH and the bound water molecules (framework). The water molecules bound to Fe atom also participate in intra-framework hydrogen bonding. These interactions bear a direct correlation with the mass losses observed in the TGA studies, indicating the strength and nature of hydrogen bond interactions present in this material.

Thermogravimetric analysis (TGA) was carried out in flowing air from room temperature up to 600°C. The results showed three different mass losses. The initial mass loss of about 4·2% around 150°C corresponds to the loss of water molecules from the

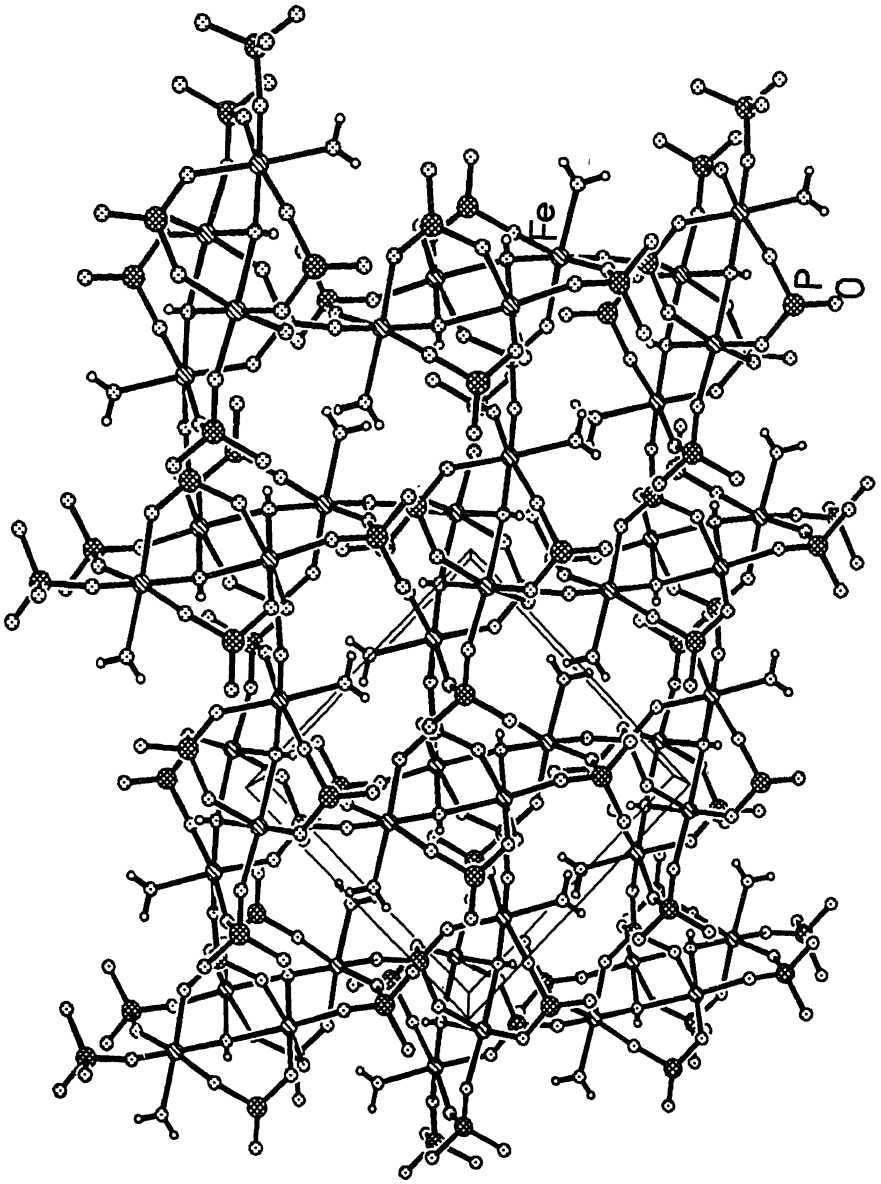

Figure 4. Structure of $[NH_4]^+[Fe_2(OH)(H_2O)(PO_4)_2]^-H_2O$ showing the one-dimensional channels along the [001] direction.

Table 4. Important hydrogen bond interactions in $[NH_4]^+[Fe_2(OH)(H_2O)(PO_4)_2]^-H_2O$.

Moiety	Distance (Å)	Moiety	Angle (°)
O(4)–H(1)	2·197(1)	O(4)–H(1)–N(1)	153·8(1)
O(8)–H(2)	2·032(1)	O(8)–H(2)–N(1)	158·8(1)
O(6)–H(3)	2·093(1)	O(6)–H(3)–N(1)	163.8(1)
O(2)–H(4)	1·965(1)	O(2)–H(4)–N(1)	165·1(1)
O(4)–H(101)	2·147(1)	O(4)–H(101)–O(100)	162·0(1)
O(7)–H(102)	2·168(1)	O(7)–H(102)–O(100)	158·1(1)
O(100)–H(10)	2·461(1)	O(100)–H(10)–O(9)	170·4(1)
O(100)–H(12)	1·915(1)	O(100)–H(12)–O(10)	169·2(1)
O(7)–H(11)[&]	2·099(1)	O(7)–H(11)–O(10)	161·5(1)

[&] Intra-framework

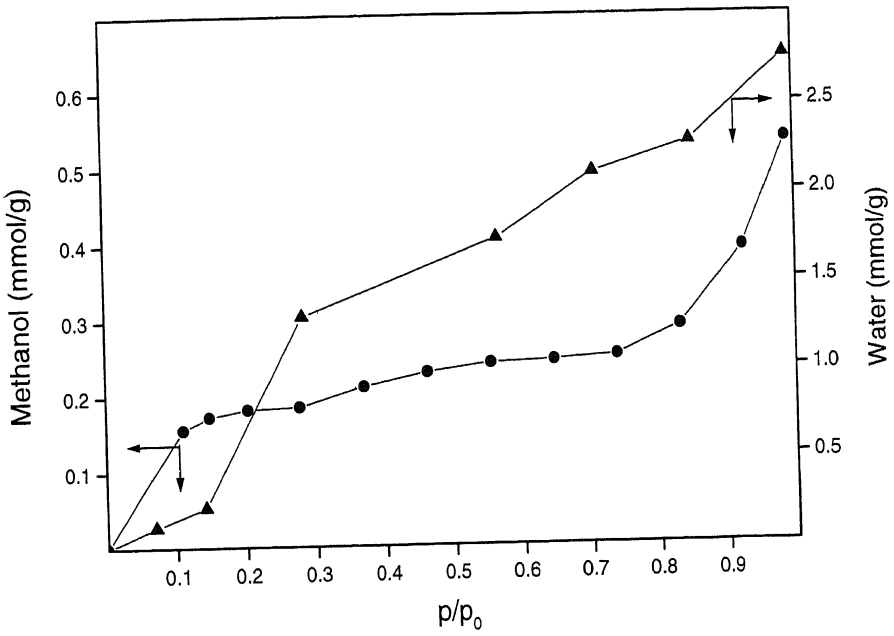

Figure 5. Adsorption isotherms at 77 K for (**a**) water and (**b**) methanol.

channels (calc. 4·7%). The second mass loss of 4·1% around 220°C corresponds to the loss of bound water molecule (calc. 4·7%) and the final broad mass loss in the region 300–400°C of 9·5% corresponds to the loss of bound –OH as well as ammonia molecule from the sample (calc. 9·3%). The powder XRD pattern of the calcined sample showed it to be weakly diffracting with a majority of the lines corresponding to the crystalline iron phosphate phase $FePO_4$. The most remarkable feature of the title compound is its ability to desorb and re-adsorb the water molecules that are present in its channels. The sample when heated at 170°C showed typical weight loss corresponding to the loss of water molecules and regained its original weight on being kept at room temperature for a couple of hours. This observation shows that the solid is capable of reversibly desorbing and adsorbing the water molecules. We have carried out systematic adsorption studies of water and methanol at 77 K on the dehydrated sample and the results are presented in figure 5. The studies indicate that the adsorption isotherm is Type I for both the molecules

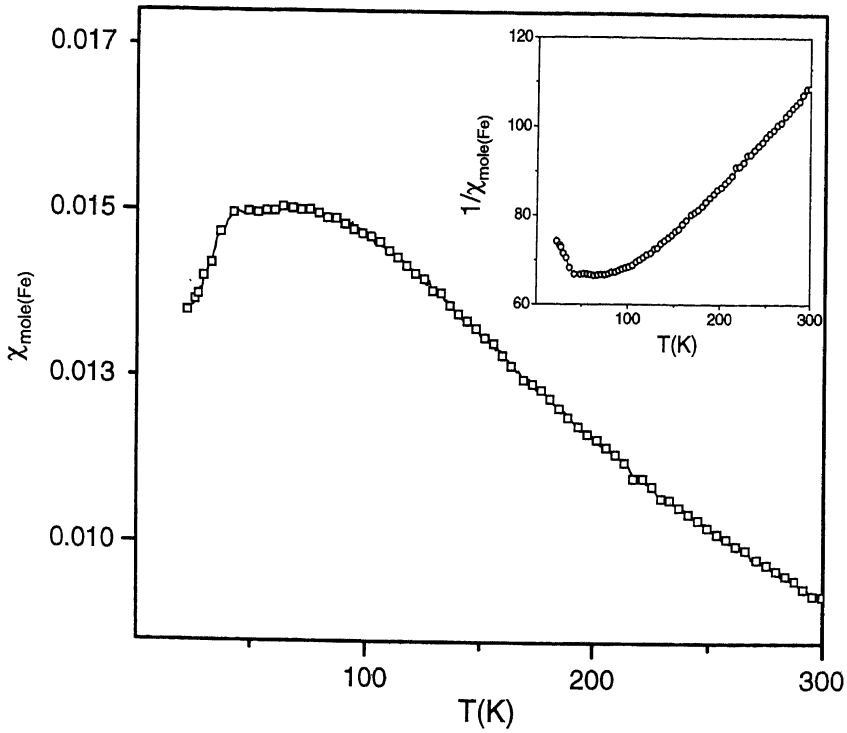

Figure 6. Magnetic susceptibility *vs* temperature plot for spheniscidite, $[NH_4]^+[Fe_2(OH)(H_2O)(PO_4)_2]^-H_2O$. Inset shows the inverse susceptibility plot.

(H_2O and CH_3OH) and correspond to one guest molecule per framework formula. The desorption–readsorption cycles did not create any perceptible change in the powder XRD of the original phase thereby indicating that the water molecules in the channels are labile. In order to probe the mobility of the NH_4^+ species we have carried out ion-exchange studies using 1·0 M NaCl solution at room temperature. The results did not show any ion-exchangeable properties indicating the hydrogen bond iterations between the NH_4^+ ions present in the channels and the framework is rather strong. We have recently found similar adsorption and ion-exchange properties in a 3-*d* tin phosphate material [18].

Magnetic susceptibility measurements in the region of 15–300 K (figure 6) indicate strong three-dimensional anti-ferromagnetic behaviour below $T_N = 22$ K ($\theta_p = -200$ K). The strong negative value of θ_p indicates predominant antiferromagnetic interactions in the compound. The calculated magnetic moment per Fe atom of 6·07 μB matches very well with the calculated value of 5·9 μB indicating all the Fe atoms are in high spin-state (Fe^{III}). Similar magnetic behaviour has also been observed by Ferey *et al* (G Ferey 1999, personal communication).

4. Conclusions

The synthetic iron phosphate mineral, spheniscidite, was synthesized under hydrothermal conditions. The solid possesses three-dimensional connectivity with two 8-membered channels arising out of the vertex linkage between the FeO_6 octahedra and PO_4 tetrahedra.

Ammonium and water molecules occupy the channels. The water molecules undergo reversible desorption–adsorption cycles without any change in structure. The dehydrated sample has adsorptive properties similar to those of aluminosilicate zeolites,

Acknowledgements

The authors thank Professor C N R Rao, FRS for his keen interest, help and encouragement. AC thanks the Council of Scientific and Industrial Research, New Delhi, for a fellowship.

References

1. Thomas J M 1994 *Angew., Chem. Intl. Ed. Engl.* **33** 913
2. Cheetham A K, Ferey G and Loiseau T 1999 *Angew., Chem. Intl. Ed. Engl.* (in press)
3. Moore P B and Shen J 1983 *Nature (London)* **306** 356
4. Bonnet P, Millet J M M, Leclercq C and Vedrine J C 1996 *J. Catal.* **158** 128, and references therein
5. Lii K H, Huang Y-F, Zima V, Huang C-Y, Lin H-M, Jiang Y-C, Liao F-L and Wang S-L 1998 *Chem. Mater.* **10** 2599
6. Cavellec M, Riou D and Ferey G 1994 *Acta Crystallogr.* **C50** 1379
7. Moore P B 1972 *Am. Mineral.* 306 356
8. a. Slieldrick G M 1986 '*SHELXS-86 Program for crystal structure determination*', University of Göttingen, Germany; b. Sheldrick G M 1990 *Acta. Crystallogr.* **A35** 467
9. Sheldrick G M, 1993 '*SHELXTL-PLUS Program for crystal structure solution and refinement*', University of Göttingen, Germany
10. Lii K-H and Huang Y-F 1997 *Chem. Commun.* 839
11. Natarajan S and Cheetham A K 1997 *J. Solid State Chem.* **139** 207
12. Neeraj S, Natarajan S and Rao C N R 1999 *Chem. Commun.* 165
13. Neeraj S, Natarajan S and Rao C N R 1999 *New J. Chem.* **23** 303
14. Neeraj S, Natarajan S and Rao C N R 1999 *Chem. Mater.* **11** 1390
15. a. Harrison W T A, Gier T E and Stucky G D 1993 *Angew. Chem. Int. Ed. Engl.* **32** 1745; b. Song T, Hursthouse M B, Chen J, Xu J, Abdul Malik K M, Jones R H, Xu R and Thomas J M 1994 *Adv. Mater.* **6** 679
16. Smith–Verdier P and Garcia–Blanco S 1980 *Z. Kristallogr.* **151** 175
17. Meier W H and Olson D H (eds) 1992 *Atlas of zeolitic structure* types (London: Butterworth-Heineman)
18. Natarajan S, Eswaramoorthy M, Cheetham A K and Rao C N R 1998 *Chem. Commun.* 1561